



OPEN

Effect of fasting and feeding on apolipoprotein A-I kinetics in pre β_1 -HDL, α -HDL, and triglyceride-rich lipoproteins

Maud Chétiveaux¹, Mikaël Croyal^{1,2}✉, Khadija Ouguerram^{1,2}, Fanta Fall¹, Laurent Flet³, Yassine Zair¹, Estelle Nobecourt^{1,4} & Michel Krempf^{1,5}

The aim of this study was to compare the kinetics of apolipoprotein (apo)A-I during fed and fasted states in humans, and to determine to what extent the intestine contributes to apoA-I production. A stable isotope study was conducted to determine the kinetics of apoA-I in pre β_1 high-density lipoprotein (HDL) and α -HDL. Six healthy male subjects received a constant intravenous infusion of ²H₃-leucine for 14 h. Subjects in the fed group also received small hourly meals. Blood samples were collected hourly during tracer infusion and then daily for 4 days. Tracer enrichments were measured by mass spectrometry and then fitted to a compartmental model using asymptotic plateau of very-low-density lipoprotein (VLDL) apoB100 and triglyceride-rich lipoprotein (TRL) apoB48 as estimates of hepatic and intestinal precursor pools, respectively. The clearance rate of pre β_1 -HDL-apoA-I was lower in fed individuals compared with fasted subjects ($p < 0.05$). No other differences in apoA-I production or clearance rates were observed between the groups. No significant correlation was observed between plasma apoC-III concentrations and apoA-I kinetic data. In contrast, HDL-apoC-III was inversely correlated with the conversion of α -HDL to pre β_1 -HDL. Total apoA-I synthesis was not significantly increased in fed subjects. Hepatic production was not significantly different between the fed group (17.17 \pm 2.75 mg/kg/day) and the fasted group (18.67 \pm 1.69 mg/kg/day). Increase in intestinal apoA-I secretion in fed subjects was 2.20 \pm 0.61 mg/kg/day. The HDL-apoA-I kinetics were similar in the fasted and fed groups, with 13% of the total apoA-I originating from the intestine with feeding.

Epidemiological studies have suggested that high-density lipoproteins (HDL) could prevent coronary heart disease but genetic cohort studies or trials investigating HDL-targeted therapies did not give strong supports to this finding¹. The metabolism and the physiological role of HDL is not fully understood and is not probably only resumed to the reverse transport of cholesterol from the macrophages to the liver². Then, the function and metabolism of HDL need to be revisited. Apolipoprotein A-I (apoA-I) constitutes the major apolipoprotein component of the HDL and is a major driver of their metabolism³. ApoA-I is produced by both the liver and the intestine and its synthesis is affected by many factors including diet^{2,3}. However, little is known about the intestinal production rate of apoA-I and the differential utilization of the HDL originating from these both sources.

Numerous kinetic studies with stable isotope tracers determined kinetic parameters of HDL-associated apoA-I. However, most of them were performed with subjects in either fasted or fed state, without direct comparisons between both study designs. Hence, the impact of fasted/fed status on HDL and apoA-I metabolism, especially within the intestine, remains not clearly understood. To address this issue, Cohn et al. analyzed HDL metabolism by exogenous labeling of apoA-I and they did not observe any change in HDL-apoA-I pool size, production rate, or catabolic rate in either the fasted or the fed state³. However, this study only analyzed mature HDL (assumed to be HDL₂ and HDL₃) which could not account for intestinal contributions.

¹CRNH-O Mass Spectrometry Core Facility, Nantes, France. ²NUN, INRA, CHU Nantes, UMR 1280, PhAN, IMAD, CRNH-O, IRS-UN-Spectrométrie de Masse-8, quai Moncoussu, 44000 Nantes, France. ³Pharmacy Department, Nantes University Hospital, Nantes, France. ⁴Nephrology Department, CHU Saint-Pierre, La Réunion, France. ⁵Clinique Bretéché, Groupe Elsan, Nantes, France. ✉email: mikaël.croyal@univ-nantes.fr

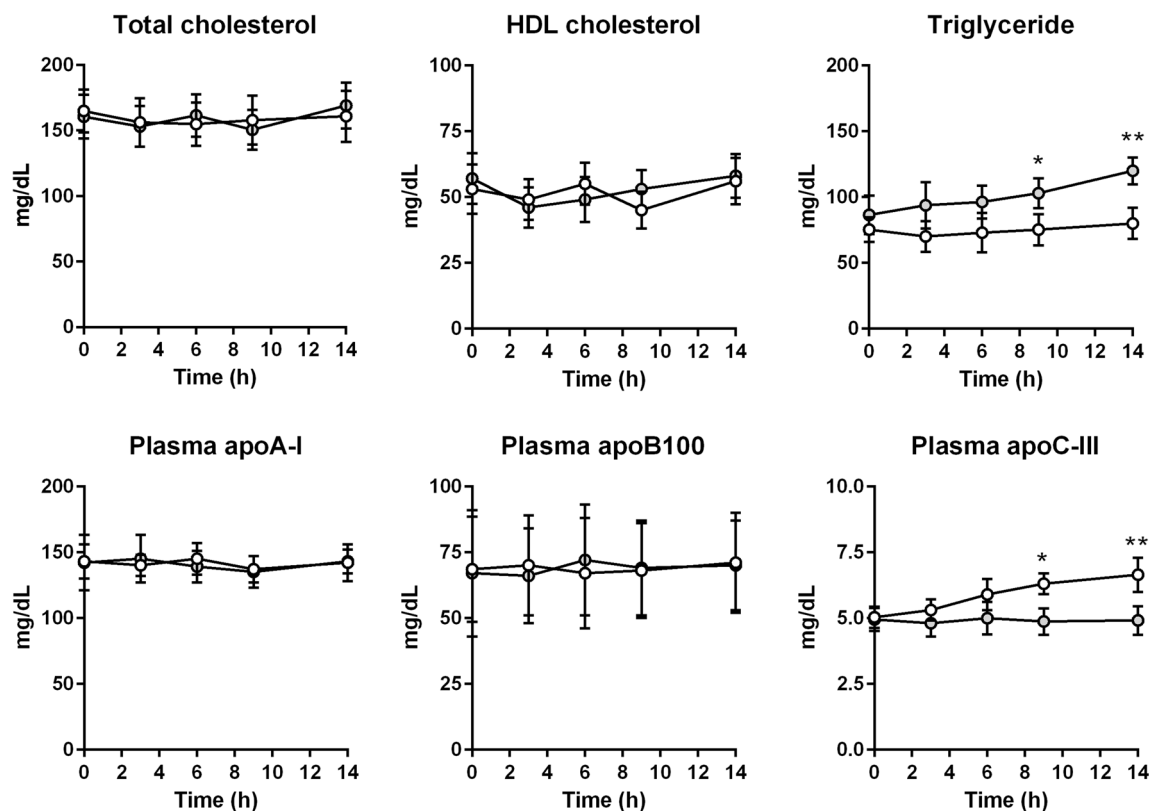


Figure 1. Evolution of main lipid parameters during the kinetic protocols. The white circles indicate the fasted state and the grey circles indicate the feeding state. Values represent means \pm SD for six subjects. * $p < 0.05$; ** $p < 0.01$ (Wilcoxon matched-pairs signed rank test).

HDL metabolism is a complex process involving precursor (pre β_1 -HDL) and mature (α -HDL) particles^{2,4}. Kinetic studies discriminating pre β_1 -HDL and α -HDL subpopulations and with a direct comparison in fasted and fed subjects have never been performed. Such studies have not been undertaken likely due to the complexity of pre β_1 -HDL metabolism, which is recycled in other HDL populations and originates from two different sources: (1) a direct synthesis from the liver and the intestine⁵, and (2) an indirect synthesis from intestine-produced postprandial triglyceride-rich lipoproteins (TRL)⁶, which have undergone hydrolysis by lipoprotein lipase^{7,8}. Of note, apolipoprotein C-III (apoC-III) inhibits TRL hydrolysis by acting on lipoprotein lipase⁹ and food intake increases apoC-III plasma concentrations^{10,11}. The pharmacological inhibition of apoC-III production with an antisense oligonucleotide dramatically increased HDL cholesterol (HDL-C) by 40% in both healthy and hypertriglyceridemic subjects¹².

We previously reported a kinetic study examining the production of pre β_1 -HDL during fasting state¹³. Here, we used the same approach to compare apoA-I kinetics in TRL, pre β_1 -HDL, and α -HDL subpopulations in healthy subjects during fasted and fed states. Our goals were to analyze the effects of food intake and therefore plasma apoC-III on HDL metabolism, and to estimate the intestinal production rate of apoA-I.

Results

Plasma lipids and apolipoprotein concentrations. As shown in Fig. 1, plasma total cholesterol (TC) concentrations did not change during the tracer infusion protocol and were similar in both the fasted and fed states. In the fasted state, plasma triglyceride (TG) concentrations remained unchanged and stable. In the fed state plasma TG concentrations were similar at baseline compared to the fasted state, then shortly increased significantly (110 ± 15 mg/dL vs. 67 ± 7 mg/dL, $p < 0.001$). HDL cholesterol (HDL-C), apolipoprotein B100 (apoB100) and apoA-I concentrations were kept constant with no difference between both experiments. While fasting did not affect plasma apoC-III concentrations (4.4 ± 0.4 mg/L at 14 h vs. 5.0 ± 0.4 mg/dL at baseline), feeding significantly increased plasma apoC-III by $30 \pm 7\%$ at 14 h ($p = 0.009$). No significant difference was found for HDL-apoC-III between both the fasted and feeding states (2.9 ± 1.3 mg/dL vs. 2.7 ± 0.9 mg/dL).

Plasma leucine enrichments. Plasma leucine enrichments increased rapidly after initial tracer injection and remained relatively constant for the 14 h duration of the studies (Fig. 2). The mean plasma leucine enrichments were lower in the fed state compared with the fasted state at their respective plateaus ($6.4 \pm 0.7\%$ vs. $9.2 \pm 0.8\%$, $p = 0.005$). As expected, the flux rate of leucine was increased with feeding (99 ± 12 μ mol/kg/h and 146 ± 15 μ mol/kg/h for fasted and fed groups, respectively, $p = 0.005$).

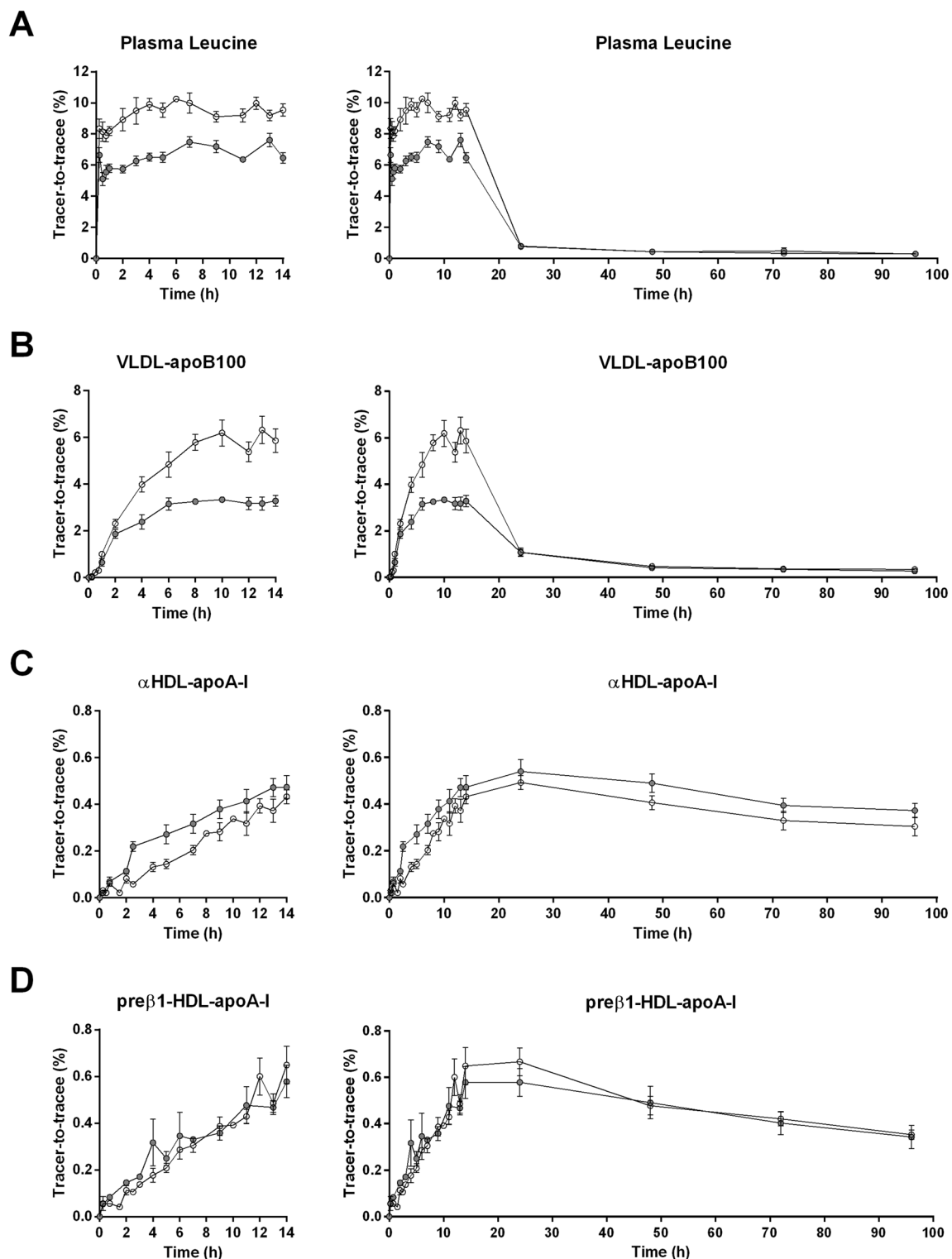


Figure 2. Enrichment of plasma leucine (A), VLDL-apoB100 (B), pre β_1 -HDL-apoA-I (C) and α -HDL-apoA-I (D) with deuterated leucine during the fasted (white circles) and fed state (grey circles) over 14 h or 96 h. Values represent means \pm SD for six subjects.

TRL-apoB48, VLDL-apoB100, HDL-apoA-I, and TRL-apoA-I enrichments. A plateau in very-low-density lipoprotein (VLDL)-apoB100 $^2\text{H}_3$ -leucine enrichments was observed in both fasted and fed groups around 8 h after the start of the tracer infusion (Fig. 2). The plateau tracer enrichment of VLDL-apoB100 was significantly lower in the fed group relative to the fasted group ($3.2 \pm 0.9\%$ vs. $6.5 \pm 1.5\%$, respectively, $p = 0.038$) and TRL-apolipoprotein B48 (apoB48) was significantly lower than that of VLDL-apoB100 ($1.4 \pm 0.5\%$ vs. $3.2 \pm 0.9\%$, $p = 0.005$) (Fig. 3). Enrichment curves of α -HDL-apoA-I did not reach a plateau and tended to be

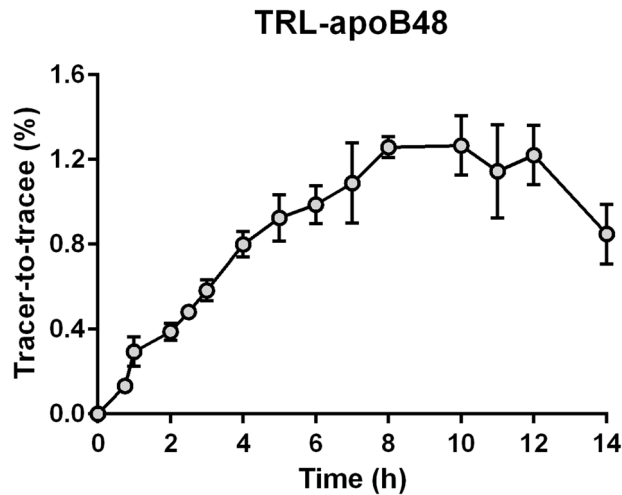


Figure 3. Enrichment of TRL-apoB48 with deuterated leucine during the fed state. Values represent means \pm SD for six subjects.

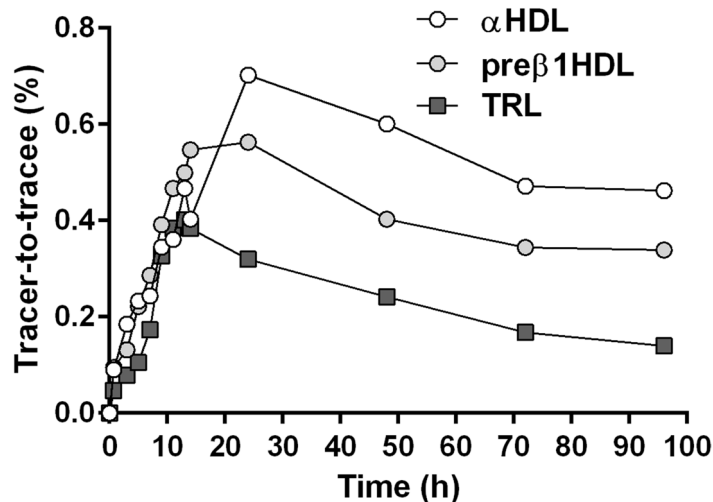


Figure 4. ApoA-I tracer/tracee ratios within TRL, pre β ₁-HDL and α -HDL fractions after a constant deuterated leucine infusion in a representative subject in a fed state.

lower in the fasted group compared to the fed group, although this difference was not significant. Pre β ₁-HDL-apoA-I enrichments were not different between both experimental groups (Fig. 2). During the infusion of the tracer, the enrichment curves were found similar for apoA-I in TRL, pre β ₁-HDL and α -HDL (Fig. 4) suggesting they are quickly exchanged and equilibrated. However, the decay curve of apoA-I enrichment upon termination of infusion was faster in TRL (0.185 ± 0.055 Atom percent excess (APE) at 96 h) than in HDL particles (0.343 ± 0.050 APE and 0.373 ± 0.030 APE at 96 h for pre β ₁-HDL and α -HDL, respectively).

Kinetic parameters within lipoprotein subclasses. In the fed group, TRL-apoA-I and TRL-apoB48 displayed similar absolute production rates (APR), while TRL-apoB48 fractional catabolic rates (FCR) were found higher than that of TRL-apoA-I ($p = 0.045$, Table 1). Exchange of apoA-I between HDL and TRL particles was identified with a net transfer of apoA-I from TRL to HDL (1.40 ± 0.48 mg/kg/day). VLDL-apoB100 kinetic parameters (catabolism, synthesis, pool size) tended to be higher in the fed group compared with the fasted group (not significant). Synthesis and clearance rates of apoA-I in the pre β ₁-HDL and α -HDL particles were not statistically different in both fasted and fed groups, except for pre β ₁-HDL-apoA-I FCR that were higher in the fasted group (Table 2, 0.447 ± 0.067 vs. 0.235 ± 0.038 pool/day, $p = 0.045$). At the feeding state, TRL- and α -HDL-apoA-I FCR were of 4.29 ± 1.09 and 0.338 ± 0.035 pool/day, respectively. The residence time (RT) of TRL-apoA-I was 0.23 days compared with 2.98 days for α -HDL-apoA-I. Hepatic apoA-I APR was estimated to be 18.67 ± 1.69 and 17.17 ± 2.75 mg/kg/day for fasted and fed groups, respectively (not significant). We could not identify any direct production of apoA-I from the intestine within the pre β ₁-HDL population. Intestinal apoA-I production could only be estimated from apoA-I secretion within the TRL isolated in the fed group, at a rate

Parameters	Fasted state	Fed state
VLDL-apoB100 FCR (pool/day)	6.94 ± 1.19	7.72 ± 1.68
VLDL-apoB100 pool (mg/kg)	76.4 ± 13	125.9 ± 16
VLDL-apoB100 APR (mg/kg/day)	7.9 ± 1.4	15.9 ± 4.8
TRL-apoB48 APR (mg/kg/day)	–	1.54 ± 0.26
TRL-apoA-I APR (mg/kg/day)	–	2.20 ± 0.61
TRL-apoB48 FCR (pool/day)	–	6.70 ± 0.93*
TRL-apoA-I FCR (pool/day)	–	4.29 ± 1.09
Absolute apoA-I transfer TRL → HDL (mg/kg/day)	–	1.40 ± 0.48

Table 1. Kinetic parameters of VLDL-apoB100 (fasted and fed states), TRL-apoB48 and TRL-apoA-I (fed state). Data from six healthy subjects are shown as the mean ± SD. * $p < 0.05$ TRL-apoB48 FCR compared with TRL-apoA-I FCR.

Parameters	Fasted state	Fed state
Conversion $\text{pre}\beta_1 \rightarrow \alpha\text{-HDL}$ (pool/day)	85.40 ± 12.68	66.56 ± 14.72
Conversion $\alpha \rightarrow \text{pre}\beta_1\text{-HDL}$ (pool/day)	4.46 ± 1.48	4.70 ± 0.91
$\text{Pre}\beta_1\text{-HDL-apoA-I FCR}$ (pool/day)	0.45 ± 0.07	0.23 ± 0.04*
$\alpha\text{-HDL-apoA-I FCR}$ (pool/day)	0.29 ± 0.03	0.34 ± 0.03
$\text{Pre}\beta_1\text{-HDL-apoA-I pool size}$ (mg/kg)	6.94 ± 1.17	7.21 ± 0.50
$\alpha\text{-HDL-apoA-I pool size}$ (mg/kg)	54.47 ± 1.44	52.94 ± 5.69
Hepatic apoA-I APR (mg/kg/day)	18.67 ± 1.69	17.17 ± 2.75
Intestinal ^a apoA-I APR (mg/kg/day)	–	2.20 ± 0.61
Total apoA-I APR (mg/kg/day)	18.67 ± 1.69	19.37 ± 2.47

Table 2. Kinetic parameters of HDL-apoA-I subclasses in fasted and fed states. Data from six healthy subjects are shown as mean ± SD for each state. * $p < 0.05$ between fasted and fed state. HDL, high-density lipoprotein; FCR, fractional catabolic rate; APR, absolute production rate. ^aEstimate of intestinal apoA-I production related to feeding. This value does not account for a basal secretion from the enterocytes in a fasted condition.

Parameters	TC	TG	HDL-C	LDL-C	Plasma apoC-III	HDL-apoC-III
TRL-apoB48 FCR	ns	ns	0.93 (0.019)	ns	ns	ns
TRL-apoB48 APR	ns	ns	ns	ns	ns	ns
TRL-apoA-I FCR	ns	ns	ns	ns	ns	ns
TRL-apoA-I APR	ns	ns	ns	ns	ns	ns
Absolute apoA-I transfer TRL → HDL	ns	ns	ns	ns	ns	ns
$\text{Pre}\beta_1\text{-HDL-apoA-I FCR}$	ns	ns	ns	ns	ns	ns
$\alpha\text{-HDL-apoA-I FCR}$	ns	ns	ns	ns	ns	ns
Conversion $\text{pre}\beta_1 \rightarrow \alpha\text{-HDL}$	ns	ns	ns	ns	ns	ns
Conversion $\alpha \rightarrow \text{pre}\beta_1\text{-HDL}$	ns	ns	ns	ns	ns	– 0.73 (0.019)
Hepatic apoA-I APR	ns	ns	ns	ns	ns	ns
Intestinal apoA-I APR	ns	ns	ns	ns	ns	ns
Total apoA-I APR	ns	ns	ns	ns	ns	ns

Table 3. Spearman correlations obtained between kinetic parameters and main plasma lipids. TRL, triglyceride-rich lipoprotein; HDL, high-density lipoprotein; FCR, fractional catabolic rate; APR, absolute production rate; TC, total cholesterol; TG, triglyceride; HDL-C, HDL cholesterol; LDL-C, LDL cholesterol; ns, not significant. Values are r coefficients (p -values).

of 2.20 ± 0.61 mg/kg/day. Therefore, $13 \pm 9\%$ of the total body apoA-I production rate could be attributed to the intestine when feeding.

Correlations. As expected, plasma TG significantly correlated with plasma apoC-III concentrations ($r = 0.70$, $p = 0.019$). As shown in Table 3, no significant correlation was observed between apoC-III plasma concentrations during the fed state and TRL-apoB48, TRL-apoA-I kinetics or intestinal apoA-I synthesis. No significant correlation was observed between any of the HDL-apoA-I kinetic parameters and apoC-III plasma concentrations for

fasted and fed groups. Of note, HDL-apoC-III was significantly and negatively correlated with the conversion of α -HDL particles to pre β_1 -HDL ($r = -0.73$, $p = 0.019$).

Discussion

In this randomized study, we investigated pre β_1 -HDL-apoA-I and α -HDL-apoA-I human kinetics in fasted and fed states and estimated the relative intestinal contribution of apoA-I total synthesis. Except for pre β_1 -HDL-apoA-I clearance rate, we observed similar kinetic data for HDL-apoA-I for both the fed and fasted states. We estimated a production rate of apoA-I from the intestine during the fed state to be around 13% of the overall production rate. Plasma apoC-III concentrations increased with feeding, but we did not observe any significant correlation between apoC-III concentrations and apoA-I kinetic data except for HDL-apoC-III that was inversely correlated with the conversion of α -HDL to pre β_1 -HDL. However, the low number of subjects enrolled here constitutes a major limitation of the study stemming primarily from the complexity of kinetic protocols.

We have adapted a model for studying apoA-I kinetics including pre β_1 -HDL¹³. Although unexpected, we had to include two pools of pre β_1 -HDL to get better fits probably because of some heterogeneity in these particles. This is a limitation of the FPLC method we have used for the sample preparation. For the fasted experiment, we assumed that the main source of apoA-I was the liver but we cannot exclude an intestinal production as suggested in animal models^{14,15}. Then, we can only estimate the production related to the meal stimulation. As a precursor pool, we used the enrichment of the intracellular hepatic leucine estimated by the enrichment plateau of VLDL-apoB100¹⁶. For the fed state model, we added intestinal apoA-I synthesis to the hepatic synthesis. For the intestinal precursor pool, we used the enrichment plateau of TRL-apoB48. TRL-apoB48 kinetic parameters were similar to those previously reported^{17–19}, validating our methods for measuring apoB48 enrichments. In this model, we assumed that intestinal apoA-I was incorporated directly into TRL particles because a direct synthesis of intestinal HDL-apoA-I could not be identified, regardless of the various models we have tested. This could represent another limitation of our study. Along the same lines, while an exchange of apoA-I between the pre β_1 -HDL, α -HDL, and TRL pools was necessary to obtain a better fit of the enrichment curves, estimates of the transfer rates of apoA-I between HDL and TRL were difficult to obtain, and large standard deviations were observed. This is another potential limitation of the model. However, for all subjects, there was an absolute net transfer of apoA-I from TRL to HDL.

We did not observe any major differences in plasma apoA-I concentrations or apoA-I kinetics between the fed and fasted states in line with a previous report²⁰. Cohn et al., with a similar study design, did not observe any change in total HDL-apoA-I kinetics in the fasted and fed states³. However, their model used the enrichment plateau of VLDL-apoB100 as a forcing function for the precursor pool, assuming that the single source of apoA-I was the liver. Although this might be true in the fasted state, the intestinal production of apoA-I is probably significant in the fed state. Using a more complex model that includes apoA-I production from the liver and the intestine, we reached the same conclusion. It can be concluded their simple model is relevant for the overall HDL-apoA-I catabolic or synthesis rates. Of note, similar ranges for data were already previously reported in fasted^{21–24} and fed^{25,26} kinetic studies, but with no direct comparison between fasting and feeding. In addition, we added information on pre β_1 -HDL-apoA-I kinetics, which revealed a decrease in the FCR with feeding, but with no related change in α -HDL mass or synthesis.

The metabolism of the pre β_1 -HDL-apoA-I is complex as they can be excreted through the kidney or recycled into the plasma (i.e. interconversion of HDL particles in the plasma compartment) via hepatic lipase, cholesterol ester transfer protein, phospholipid transfer protein, and phospholipids or HDL-apoM²⁷. Most of these factors could be modulated through diet and their specific roles deserve further investigations.

To the best of our knowledge, three studies have looked at the kinetic metabolism of pre β_1 -HDL-apoA-I and mature HDL with an endogenous labeling of apoA-I with a stable isotope tracer. Two studies have used a constant infusion of the tracer and blood sample collection over 10 h to 14 h in fasted subjects^{13,28} while a large bolus injection of the tracer over 10 min was used in the last one associated with blood sampling over 96 h in non-fasted patients²⁹. Similar kinetic data were observed in the first two studies but controversial results were reported in the third one. This could be attributed to the different study designs and blood sample collection or a larger number of analyzed HDL particles but the modeling is probably the main reason of this discrepancy. Although a clear relation between precursor and product was reported in monkeys between pre β_1 -HDL-apoA-I and α -HDL-apoA-I with exogenous labeled native HDL with radiotracers³⁰, the authors challenged the canonical stepwise enlargement and contraction model for HDL metabolism. From the similarity of the tracer enrichment curves in the different particles, as we have also observed in this study, they suggested a direct and large entry of apoA-I into the mature HDL. Their conclusion can be challenged because the subjects were not fasted and they did not take into account any exchanges with the TRL-apoA-I. In the different models they have tested, in one of them close to our approach, a good fit was also observed. Nevertheless, they decided to discard this model because of its simplicity. Finally, they assumed that the similarity of the tracer enrichment curves means a direct entry in each particle. This could be also related to very fast exchanges and equilibrium between the circulating particles while the labeled protein is slowly synthesized as apoA-I. A recent *in vitro* study has studied the conversion rate of nascent to mature HDL in BHK-ABCA1 cells²⁹. The conversion was solely to mature HDL and very fast ($t_{1/2} < 10$ min) and in a range similar of the pre β_1 -HDL-apoA-I residence time we have observed. Beside these discrepancies, these results altogether raised a limit of the endogenous labeling of slow synthesis proteins incorporated in circulating carriers with fast exchanges and turnover rates. New study designs and modeling should be probably proposed in this particular situation.

Our model suggests the increased intestinal apoA-I production related to meal stimulation must be first incorporated into TRL particles and then exchanged with mature HDL. This assumption may represent a limitation of our model. Studies in animal models have observed a synthesis of apoA-I and HDL within the enterocytes

accounting for 30% of the circulating pool¹⁴ but evidences supporting a direct synthesis of HDL particles from the intestine in humans are not strong. Pre β_1 -HDL and α -HDL have been identified in the peripheral lymph³¹. However, due to a filtration process, the peripheral lymph HDL profile seems to reflect the plasma HDL profile and, in contrast to the rat model, nascent HDL particles were not observed in human samples of thoracic duct lymph^{32,33}.

We estimated that intestinal apoA-I synthesis, shuttling through TRL particles, accounts for approximately 13% of the total apoA-I production with a meal stimulation. Green et al. estimated that about 50% of apoA-I originated from the intestine in chyluric patients, but this is a disease-state model³⁴. Anderson et al. assumed that only apoA-I in association with lymph chylomicrons represents the contribution of intestinal synthesis, and was estimated to be around 26% in patients with thoracic duct drainage³². Again, this result could be challenged because of the apoA-I filtration process from plasma to lymph. Consistent with our data, Ikewaki et al. estimated that the intestine contributed to 10% of the total apoA-I pool by using dual stable isotope and radiotracer infusion³⁵. However, when Velez-Carrasco et al.²⁵ performed a single tracer infusion study of apoA-I kinetics within TRL and mature HDL (but not pre β_1 -HDL) in a fed state, they found no exchange of apoA-I between HDL and TRL. Furthermore, they did not identify a direct catabolism of apoA-I from TRL or a direct production of mature HDL from the intestine. Although their measured rates of total apoA-I synthesis and catabolism were similar to our data, they estimated that intestinal apoA-I synthesis reflects only 0.15% of the total synthesis of apoA-I. This large discrepancy could be explained by differences in the compartmental analysis models, experimental protocol lengths, and experimental diets or, as acknowledged by the authors, some very fast exchanges not able to be captured with the experimental protocol. An accurate measurement of intestinal apoA-I synthesis would have required a specific labeling within the intestine. However, specific tracers of protein synthesis targeting only this tissue have not yet been identified.

The increase in plasma apoC-III concentrations upon feeding was previously reported and likely reflects an increase in apoC-III synthesis^{10,11}. ApoC-III is an inhibitor of lipoprotein and hepatic lipases and increases the assembly and production of VLDL from the liver^{36,37}. Overall, apoC-III increases plasma TG levels⁹. Previous kinetic studies reported a significant inverse correlation between HDL-apoA-I catabolic rates and HDL-apoC-III concentrations³⁸. In line with this report, we found an inverse correlation between HDL-apoC-III and the conversion of α -HDL to pre β_1 -HDL particles. However, whether this finding is related to a direct effect of apoC-III on apoA-I metabolism, or an indirect effect due to changes in the TG content of HDL or plasma remains unknown. Recent studies with an antisense oligonucleotide showed an increase in HDL-C associated with a sharp reduction in plasma apoC-III¹². Therefore, decreases in plasma apoA-I and HDL-C levels could be expected with the increase in apoC-III levels observed with feeding but we did not observe this lipid profile during the feeding experiment. Furthermore, no significant correlation was found between plasma apoC-III concentration and catabolic rates of apoA-I in mature or pre β_1 -HDL. The limited absolute increase in plasma apoC-III concentrations and the small number of subjects in this study could account for this lack of association. Kinetic studies with apoC-III inhibitors would be more appropriate to address this question.

In conclusion, we did not observe any major differences in global apoA-I kinetic parameters (synthesis and catabolism) between the fed and fasted states. This observation validates the comparison of kinetic data concerning apoA-I obtained from different studies, regardless of differences in their experimental protocols and food intake. Until a method of direct and specific labeling of intestinal apoA-I will be established, our approach and model, albeit some limitations, provide a reasonable estimate of intestinal apoA-I synthesis stimulated by a meal. Finally, this study raised some limitations for the kinetic study of very fast turnover lipoproteins with an endogenous tracer labeling.

Materials and methods

Patients. Six healthy male subjects (age: 26.3 ± 5.7 years, body mass index: 21.1 ± 2.5 kg/m²) with normal plasma lipid concentrations (TC: 164 ± 30 mg/dL, TG: 75 ± 27 mg/dL, HDL-C: 53 ± 10 mg/dL, low-density-lipoprotein cholesterol (LDL-C): 93 ± 32 mg/dL, apoA-I: 143 ± 13 mg/dL, and apoB100: 69 ± 20 mg/dL) and without medication were included in a crossover design study. They were submitted to two explorations within 2 weeks described later as the fasted and feeding protocols. The order of the first exploration (fasted or feeding) was randomly assigned. The experimental protocol was approved by the ethics committee of Nantes University Hospital. A written consent was obtained from each volunteer before inclusion in the study (CPPRB Pays de Loire, reference 0266). All methods were carried out in accordance with guidelines and regulations of the ethics committee of Nantes University Hospital.

Experimental design. After an overnight fasting (12 h), subjects received a primed bolus of ²H₃-leucine at 10 μ mol/kg (99.8 atom %; Cambridge Isotope, MA, USA), immediately followed by a constant infusion at 10 μ mol/kg/h for 14 h. For the feeding protocol, a 2,200-kcal meal composed of Slim Fast, cheese, and toasted bread was divided into 16 equal portions. Each meal portion was carefully weighed and contained 44% carbohydrate, 15% protein, and 41% fat by calories corresponding to 1/18 of the total calorie intake. After the 12 h overnight fasting, subjects received a meal portion at 2 h and 1 h before bolus tracer injection ($t=0$ h). Then, one meal portion was given every hour during tracer injection ($t=0$ h to 13 h). Venous blood samples (5 mL) were drawn into EDTA tubes (Venoject, Paris, France) at baseline ($t=0$ h), every 15 min during the first hour, every 30 min during the next 2 h, and then hourly until the completion of the study. All blood samples were withdrawn before food intakes. The infusion protocol was identical for the fasted state experiment, but no meal portions were given (subjects were given free access to water). Over the next 4 days, fasted and fed subjects resumed their normal diets, and a daily blood sample was collected ($t=24$ h, 48 h, 72 h, and 96 h).

Sample preparation and storage. Immediately after blood collection, plasma was separated by centrifugation for 30 min at 4 °C. Sodium azide, an inhibitor of bacterial growth, and a protease inhibitor were added to plasma samples at final concentrations of 1.5 and 0.5 mM, respectively. All samples were stored at – 80 °C until use.

ApoC-III measurements. ApoC-III was quantified by trypsin proteolysis and liquid chromatography-tandem mass spectrometry analysis of signature peptides as previously described and validated³⁹.

Isolation of HDL subclasses. HDL subclass separation was performed by fast protein liquid chromatography (FPLC) on a Superdex 200 h 10/30 column (Amersham Pharmacia Biotech Inc., Orsay, France). Elution buffer contained 1 mM EDTA, 154 mM NaCl, and 0.02% NaN₃ and was pre-filtered through a 0.22- μ m GV membrane filter (Duroapore, Millipore, Billerica, MD, USA). Plasma samples (200 μ L) were injected, eluted at a flow rate of 0.35 mL/min, and 0.2-mL fractions were collected. ApoA-I contents in FPLC fractions were measured by immunoturbidimetry. Details on FPLC profiles and the purity of collected fractions have been described previously⁴⁰. To only analyze pure HDL subclasses, 10 fractions, assumed to be a mixture of α -HDL and pre β ₁-HDL, were not considered. With this exclusion criterion, 52% of total plasma apoA-I was recovered, with 89% of apoA-I in α -HDL and 11% in pre β ₁-HDL. To determine the concentrations of apoA-I within pre β ₁- and α -HDL subpopulations, we multiplied these percentages (89% for α -HDL and 11% for pre β ₁-HDL) by the total plasma concentration of apoA-I. To confirm the purity of the subclasses, non-denaturing two-dimensional polyacrylamide gel electrophoresis (PAGE) was performed on α -HDL and pre β ₁-HDL FPLC fractions. After electrophoresis, lipoproteins were transferred onto a nitrocellulose membrane. An anti-apoA-I antibody was applied to confirm that pre β ₁-HDL particles were not found in the α -HDL sample and reciprocally, as previously described⁴⁰.

Isolation of TRL by ultracentrifugation. The density of plasma was adjusted to 1.006 g/mL with a NaCl solution. Very-low-density lipoproteins (VLDL) were isolated by ultracentrifugation using a LKB ultracentrifuge with a RP55T rotor at 40,000 rpm for 24 h at 4 °C. For plasma from the fed group, this fraction contained chylomicrons and, therefore, was referred to as the TRL fraction. VLDL-apoB100 concentrations were measured by immunoturbidimetry and TRL-apoB48 concentrations were determined by gas chromatography-mass spectrometry (GC-MS) as previously described⁴¹.

Isolation and preparation of apolipoproteins. ApoA-I was resolved from the purified HDL subclass preparations by a 4–20% gradient sodium dodecylsulfate (SDS)-PAGE. ApoB100 and apoB48 were resolved from the VLDL and TRL preparations using a 4–10% gradient SDS-PAGE. These apolipoproteins were first identified by immunoblotting with an antibody against human apoB48/B100 (Biodesign, Saco, ME). In parallel, apolipoproteins were also isolated by SDS-PAGE and stained with Coomassie Brilliant Blue R 250 (Sigma Aldrich, Saint-Quentin Fallavier, France). Apolipoproteins were identified by comparing migration distances with known molecular weight standards (electrophoresis calibration kit, Pharmacia LKB, Biotechnology Inc., Piscataway, NJ, USA). The apoA-I, apoB100, and apoB48 bands were then excised from the polyacrylamide gels and hydrolyzed for 24 h in 4 N HCl at 110 °C^{16,23}. Hydrolysates were used to determine tracer-to-tracee ratios.

Measurements of tracer enrichments. Hydrolysates were dried under nitrogen and amino acids were purified by cation exchange chromatography using a Dowex 50WX8-200 resin (Sigma Aldrich). Amino acids were esterified with propanol/acetyl chloride and derivatized using heptafluorobutyric anhydride (HFBA, Fluka, Saint-Quentin Fallavier, France). GC-MS enrichment measurements were performed on a 5890A gas chromatograph connected with a 5971A quadrupole mass spectrometer (Hewlett-Packard, Palo Alto, CA). The isotopic ratio was determined by the selected ion-monitoring mode at mass-to-charge ratios of 282 and 285 for endogenous and labeled leucine, respectively^{13,40}.

Model assumptions and kinetic analysis. Kinetic analysis of tracer-to-tracee ratios was achieved by using computer software for simulation, analysis, and modeling (SAAM II, version 1.0.1, Resource Facility for Kinetic Analysis, Department of Bioengineering, SAAM Institute, Seattle, WA, USA). Different models were tested and we selected two of them for the fasted and fed states giving the best goodness-of-fit measures according to Akaike Information Criterion. The multi-compartmental model used for studying apoA-I metabolism is shown in Fig. 5A for the fasted experiment¹³. This model was adapted (Fig. 5B) for the fed experiment. Compartments 1 and 4 represent apolipoprotein precursor pools defined respectively by a forcing function representing asymptotic enrichment plateau from either VLDL-apoB100, that only originates from the liver (fasted and fed experiments), or TRL-apoB48, the truncated form of apoB100 that only originates from the intestine (fed experiment only). Intracellular delay compartments represent the time required for apoA-I synthesis and secretion from the liver and intestine. Compartments 2 and 3 are tracer-to-tracee enrichment curves of apoA-I within the pre β ₁-HDL and α -HDL populations, respectively. The model allowed reversible transfer of apoA-I between HDL subclasses. Presumption of heterogeneity of pre β ₁-HDL generated a better fit to the data, but did not dramatically affect the kinetic parameters. Then, pools 2 and 20 were associated with the apoA-I-pre β ₁-HDL tracer-to-tracee ratio. Their pool sizes were calculated by the model assuming their sums were equal to the total apoA-I-pre β ₁-HDL pool. In the fed experiment model (Fig. 5B), compartment 5 represents TRL-associated apoA-I (tracer-to-tracee ratio and mass). Exchange of apoA-I between the TRL and HDL compartments and direct catabolism of apoA-I from the TRL and HDL compartments were included in the model to obtain a better fit. The apoB48 kinetics were obtained from a simple model with two compartments. Tracer-to-tracee ratios of

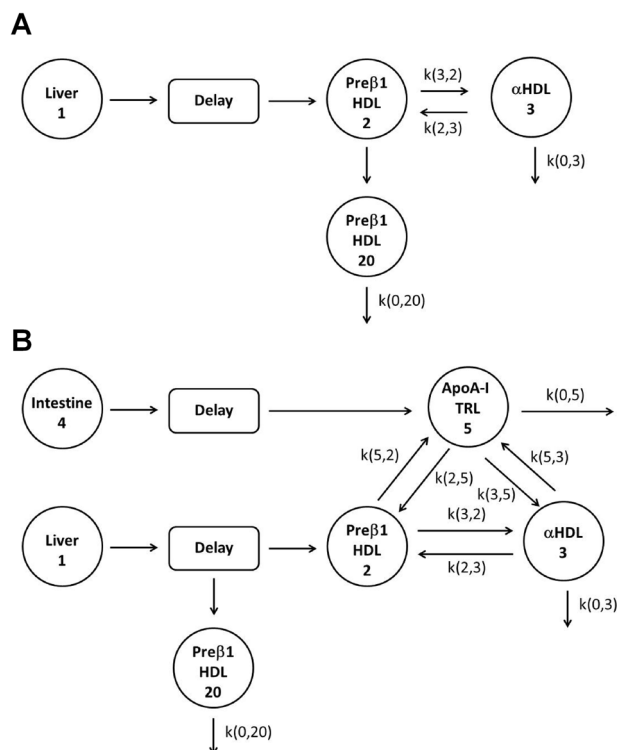


Figure 5. Multi-compartmental model used to analyze kinetics of apolipoprotein A-I (apoA-I) in the fasting (A) and the fed (B) states.

VLDL-apoB100 were fitted to a mono-exponential function, defined as $A(t) = A_p(1 - e^{-k(t-d)})$, where $A(t)$ is the apolipoprotein enrichment at time t , A_p is the enrichment of the tissue precursor amino acid pool from which the protein was derived (estimated from VLDL-associated apoB100 enrichment curve at plateau), d is the delay between the beginning of the experiment and the appearance of tracer in apolipoprotein, and k is the fractional synthetic rate (FSR) of apolipoprotein. The fractional production rate (FPR), defined as the proportion of apoA-I entering the pool per unit time (pool/day), and the absolute production rate (APR), defined as the amount of apoA-I entering the pool per unit time (mg/kg/day), were estimated. APR is the product of the FPR and the pool size of apoA-I in each HDL subclass. The apoA-I pool size (mg/kg) was calculated by multiplying the mean HDL subclass apoA-I concentration by 0.045 (L/kg), based on an assumed plasma volume of 4.5% of body weight⁴². The apoA-I pool size was considered to be constant, as no significant variation was observed between measurements made at different sampling times in the fasted and fed states. Under these steady-state conditions, FPR equals the fractional catabolic rate (FCR). Rates for apoA-I clearance and recycling within the HDL subclasses or apoA-I exchange between HDL and TRL were estimated and expressed in units of pool/day. The clearance rate reflects the direct removal of apoA-I [$k(0,20)$; $k(0,3)$; $k(0,5)$ in Fig. 5]. The residence time (RT) was $1/\text{FCR}$. ApoA-I recycling corresponded to conversion between pre β_1 -HDL and α -HDL [$k(3,2)$; $k(2,3)$]. ApoA-I exchange between HDL and TRL was characterized by four parameters [$k(2,5)$; $k(5,2)$; $k(3,5)$; $k(5,3)$], but was expressed as the absolute apoA-I transfer rate between TRL and HDL (mg/kg/day).

Statistical analysis. Data are reported as the mean \pm standard deviation (SD), unless otherwise specified. The Wilcoxon matched-pairs signed rank test (significance at $p < 0.05$) was used to determine differences between groups using GraphPad Prism software (version 6.0, GraphPad Software Inc., La Jolla, CA, USA). Correlations were evaluated by the Spearman test.

Data availability

The datasets analyzed during the current study are available from the corresponding author on reasonable request.

Received: 21 November 2019; Accepted: 3 August 2020

Published online: 24 September 2020

References

1. Hegele, R. A. *et al.* Rare dyslipidaemias, from phenotype to genotype to management: A European Atherosclerosis Society task force consensus statement. *Lancet Diabetes Endocrinol.* **8**, 50–67 (2020).
2. Rye, K.-A. & Barter, P. J. Formation and metabolism of prebeta-migrating, lipid-poor apolipoprotein A-I. *Arterioscler. Thromb. Vasc. Biol.* **24**, 421–428 (2004).

3. Cohn, J. S., Wagner, D. A., Cohn, S. D., Millar, J. S. & Schaefer, E. J. Measurement of very low density and low density lipoprotein apolipoprotein (Apo) B-100 and high density lipoprotein Apo A-I production in human subjects using deuterated leucine. Effect of fasting and feeding. *J. Clin. Investig.* **85**, 804–811 (1990).
4. Rye, K. A., Clay, M. A. & Barter, P. J. Remodelling of high density lipoproteins by plasma factors. *Atherosclerosis* **145**, 227–238 (1999).
5. Danielsen, E. M., Hansen, G. H. & Poulsen, M. D. Apical secretion of apolipoproteins from enterocytes. *J. Cell Biol.* **120**, 1347–1356 (1993).
6. Cohn, J. S. *et al.* Contribution of apoB-48 and apoB-100 triglyceride-rich lipoproteins (TRL) to postprandial increases in the plasma concentration of TRL triglycerides and retinyl esters. *J. Lipid Res.* **34**, 2033–2040 (1993).
7. Schaefer, E. J. *et al.* Transfer of human lymph chylomicron constituents to other lipoprotein density fractions during in vitro lipolysis. *J. Lipid Res.* **23**, 1259–1273 (1982).
8. Jiang, X. C. *et al.* Targeted mutation of plasma phospholipid transfer protein gene markedly reduces high-density lipoprotein levels. *J. Clin. Investig.* **103**, 907–914 (1999).
9. Kohan, A. B. Apolipoprotein C-III: a potent modulator of hypertriglyceridemia and cardiovascular disease. *Curr. Opin. Endocrinol. Diabetes Obes.* **22**, 119–125 (2015).
10. Desroches, S. *et al.* Kinetics of plasma apolipoprotein C-III as a determinant of diet-induced changes in plasma triglyceride levels. *Eur. J. Clin. Nutr.* **62**, 10–17 (2008).
11. Huff, M. W., Fidge, N. H., Nestel, P. J., Billington, T. & Watson, B. Metabolism of C-apolipoproteins: kinetics of C-II, C-III1 and C-III2, and VLDL-apolipoprotein B in normal and hyperlipoproteinemic subjects. *J. Lipid Res.* **22**, 1235–1246 (1981).
12. Gaudet, D. *et al.* Antisense Inhibition of Apolipoprotein C-III in Patients with Hypertriglyceridemia. *N. Engl. J. Med.* **373**, 438–447 (2015).
13. Chétiveaux, M. *et al.* New model for kinetic studies of HDL metabolism in humans. *Eur. J. Clin. Invest.* **34**, 262–267 (2004).
14. Brunham, L. R. *et al.* Intestinal ABCA1 directly contributes to HDL biogenesis in vivo. *J. Clin. Investig.* **116**, 1052–1062 (2006).
15. Otis, J. P., Shen, M.-C., Caldwell, B. A., Reyes Gaido, O. E. & Farber, S. A. Dietary cholesterol and apolipoprotein A-I are trafficked in endosomes and lysosomes in the live zebrafish intestine. *Am. J. Physiol. Gastrointest. Liver Physiol.* **316**, G350–G365 (2019).
16. Maugeais, C. *et al.* A minimal model using stable isotopes to study the metabolism of apolipoprotein B-containing lipoproteins in humans. *Diabetes Metab.* **22**, 57–63 (1996).
17. Lichtenstein, A. H. *et al.* Measurement of human apolipoprotein B-48 and B-100 kinetics in triglyceride-rich lipoproteins using [5,5,5-²H₃]leucine. *J. Lipid Res.* **33**, 907–914 (1992).
18. Vélez-Carrasco, W. *et al.* Human apolipoprotein A-I kinetics within triglyceride-rich lipoproteins and high density lipoproteins. *J. Lipid Res.* **40**, 1695–1700 (1999).
19. Welty, F. K., Lichtenstein, A. H., Barrett, P. H., Dolnikowski, G. G. & Schaefer, E. J. Human apolipoprotein (Apo) B-48 and ApoB-100 kinetics with stable isotopes. *Arterioscler. Thromb. Vasc. Biol.* **19**, 2966–2974 (1999).
20. Cohn, J. S., McNamara, J. R., Cohn, S. D., Ordovas, J. M. & Schaefer, E. J. Plasma apolipoprotein changes in the triglyceride-rich lipoprotein fraction of human subjects fed a fat-rich meal. *J. Lipid Res.* **29**, 925–936 (1988).
21. Batal, R. *et al.* Familial HDL deficiency characterized by hypercatabolism of mature apoA-I but not proapoA-I. *Arterioscler. Thromb. Vasc. Biol.* **18**, 655–664 (1998).
22. Schaefer, J. R. *et al.* Metabolic basis of high density lipoproteins and apolipoprotein A-I increase by HMG-CoA reductase inhibition in healthy subjects and a patient with coronary artery disease. *Atherosclerosis* **144**, 177–184 (1999).
23. Frénais, R. *et al.* High density lipoprotein apolipoprotein AI kinetics in NIDDM: a stable isotope study. *Diabetologia* **40**, 578–583 (1997).
24. Frénais, R. *et al.* Apolipoprotein A-I kinetics in heterozygous familial hypercholesterolemia: a stable isotope study. *J. Lipid Res.* **40**, 1506–1511 (1999).
25. Velez-Carrasco, W. *et al.* Apolipoprotein A-I and A-II kinetic parameters as assessed by endogenous labeling with [(2)H(3)]leucine in middle-aged and elderly men and women. *Arterioscler. Thromb. Vasc. Biol.* **20**, 801–806 (2000).
26. Pont, F., Duvillard, L., Florentin, E., Gambert, P. & Vergès, B. High-density lipoprotein apolipoprotein A-I kinetics in obese insulin resistant patients. An in vivo stable isotope study. *Int. J. Obes. Relat. Metab. Disord. J. Int. Assoc. Study Obes.* **26**, 1151–1158 (2002).
27. Rye, K.-A. & Barter, P. J. Regulation of high-density lipoprotein metabolism. *Circ. Res.* **114**, 143–156 (2014).
28. Li, X., Stolinski, M. & Umpleby, A. M. Development of a method to measure preβHDL and αHDL apoA-I enrichment for stable isotopic studies of HDL kinetics. *Lipids* **47**, 1011–1018 (2012).
29. Xu, B., Gillard, B. K., Gotto, A. M., Rosales, C. & Pownall, H. J. ABCA1-derived nascent high-density lipoprotein-apolipoprotein AI and lipids metabolically segregate. *Arterioscler. Thromb. Vasc. Biol.* **37**, 2260–2270 (2017).
30. Colvin, P. L., Moriguchi, E., Barrett, P. H., Parks, J. S. & Rudel, L. L. Small HDL particles containing two apoA-I molecules are precursors in vivo to medium and large HDL particles containing three and four apoA-I molecules in nonhuman primates. *J. Lipid Res.* **40**, 1782–1792 (1999).
31. Nanjee, M. N. *et al.* Composition and ultrastructure of size subclasses of normal human peripheral lymph lipoproteins: quantification of cholesterol uptake by HDL in tissue fluids. *J. Lipid Res.* **42**, 639–648 (2001).
32. Anderson, D. W. *et al.* Transport of apolipoproteins A-I and A-II by human thoracic duct lymph. *J. Clin. Investig.* **67**, 857–866 (1981).
33. Green, P. H., Tall, A. R. & Glickman, R. M. Rat intestine secretes discoid high density lipoprotein. *J. Clin. Investig.* **61**, 528–534 (1978).
34. Green, P. H., Glickman, R. M., Saudek, C. D., Blum, C. B. & Tall, A. R. Human intestinal lipoproteins. Studies in chyluric subjects. *J. Clin. Investig.* **64**, 233–242 (1979).
35. Ikewaki, K. *et al.* Evaluation of apoA-I kinetics in humans using simultaneous endogenous stable isotope and exogenous radiotracer methods. *J. Lipid Res.* **34**, 2207–2215 (1993).
36. Cohn, J. S., Patterson, B. W., Uffelman, K. D., Davignon, J. & Steiner, G. Rate of production of plasma and very-low-density lipoprotein (VLDL) apolipoprotein C-III is strongly related to the concentration and level of production of VLDL triglyceride in male subjects with different body weights and levels of insulin sensitivity. *J. Clin. Endocrinol. Metab.* **89**, 3949–3955 (2004).
37. Sundaram, M. *et al.* Expression of apolipoprotein C-III in McA-RH7777 cells enhances VLDL assembly and secretion under lipid-rich conditions. *J. Lipid Res.* **51**, 150–161 (2010).
38. Le, N. A., Gibson, J. C. & Ginsberg, H. N. Independent regulation of plasma apolipoprotein C-II and C-III concentrations in very low density and high density lipoproteins: implications for the regulation of the catabolism of these lipoproteins. *J. Lipid Res.* **29**, 669–677 (1988).
39. Croyal, M. *et al.* Stable Isotope Kinetic Study of ApoM (Apolipoprotein M). *Arterioscler. Thromb. Vasc. Biol.* **38**, 255–261 (2018).
40. Chétiveaux, M. *et al.* The differential apoA-I enrichment of prebeta1 and alphaHDL is detectable by gel filtration separation. *J. Lipid Res.* **43**, 1986–1993 (2002).
41. Beghin, L. *et al.* Measurement of apolipoprotein B concentration in plasma lipoproteins by combining selective precipitation and mass spectrometry. *J. Lipid Res.* **41**, 1172–1176 (2000).
42. Dagher, F. J., Lyons, J. H., Finlayson, D. C., Shamsai, J. & Moore, F. D. Blood volume measurement: A critical study prediction of normal values: controlled measurement of sequential changes: choice of a bedside method. *Adv. Surg.* **1**, 69–109 (1965).

Acknowledgments

The authors thank the staff of the Clinical Investigation Center of the University Hospital in Nantes, especially Eliane Hiverneau for their invaluable helps with patients and blood collection. The authors also thank Stéphanie Billon-Crossouard and Audrey Aguesse for their technical assistance. This study was supported by grants from the department of Clinical Research of Nantes Hospital (Direction de la Recherche Clinique) and Astra Zeneca Company.

Author contributions

M.Ch., M.K. and E.N. conceived and designed research; M.Ch., M.Cr., K.O., F.F., L.F. and Y.Z. performed experiments and laboratory analyses; M.Ch., M.Cr., K.O. and M.K. analyzed data; M.Ch., M.Cr., M.K. and E.N. edited and revised manuscript; all authors approved final version of manuscript.

Competing interests

The authors declare no competing interests.

Additional information

Correspondence and requests for materials should be addressed to M.C.

Reprints and permissions information is available at www.nature.com/reprints.

Publisher's note Springer Nature remains neutral with regard to jurisdictional claims in published maps and institutional affiliations.



Open Access This article is licensed under a Creative Commons Attribution 4.0 International License, which permits use, sharing, adaptation, distribution and reproduction in any medium or format, as long as you give appropriate credit to the original author(s) and the source, provide a link to the Creative Commons licence, and indicate if changes were made. The images or other third party material in this article are included in the article's Creative Commons licence, unless indicated otherwise in a credit line to the material. If material is not included in the article's Creative Commons licence and your intended use is not permitted by statutory regulation or exceeds the permitted use, you will need to obtain permission directly from the copyright holder. To view a copy of this licence, visit <http://creativecommons.org/licenses/by/4.0/>.

© The Author(s) 2020